PHYSICAL REVIEW B **71**, 220411(R) (2005)

Unconventional magnetic properties of the weakly ferromagnetic metal $BaIrO_3$

M. L. Brooks,[1] S. J. Blundell,[1] T. Lancaster,[1] W. Hayes,[1] F. L. Pratt,[2] P. P. C. Frampton,[3] and P. D. Battle[3]
[1]*Clarendon Laboratory, University of Oxford, Parks Road, Oxford OX1 3PU, United Kingdom*
[2]*ISIS Muon Facility, ISIS, Chilton, Oxfordshire OX11 0QX, United Kingdom*
[3]*Inorganic Chemistry Laboratory, University of Oxford, South Parks Road, Oxford OX1 3QR, United Kingdom*
(Received 6 April 2005; published 29 June 2005)

We present experimental evidence for small-moment magnetism below the ferromagnetic transition temperature ($T_{c3}=183$ K) in the quasi-one-dimensional metal $BaIrO_3$. Further, we identify rearrangement of the *local* magnetic moment distribution, which leaves the *bulk* magnetization unchanged, at the Mott-like transition ($T_{c1}=26$ K). These results are only possible via muon-spin relaxation (μSR) techniques, since neutron scattering studies are hindered by the large absorption of neutrons by Ir. The low-temperature characteristics of this compound, as revealed by μSR, are unconventional, and suggest that its magnetic properties are driven by changes occurring at the Fermi surface due to the formation of a charge-density wave state.

DOI: 10.1103/PhysRevB.71.220411 PACS number(s): 76.75.+i, 75.30.−m, 75.50.−y, 71.45.Lr

The extended nature of the *d* orbitals that are present in the second and third transition series oxides means that crystalline field splittings are enhanced and there is significant *d-p* hybridization between the transition metal ion and the surrounding oxygen octahedron. This leads to strong coupling between the electronic, lattice, and orbital degrees of freedom, which results in a wide variety of ground states. Complex phase diagrams result and the electronic properties of these materials may be dramatically altered by small structural changes.[1,2] $BaIrO_3$ is a particularly interesting example: it shows weak ferromagnetism with an unexpectedly high Curie temperature, charge-density-wave (CDW) formation, and a temperature-driven transition from a bad-metal state to an insulating ground state.[3]

The crystal structure of $BaIrO_3$ features three face-sharing IrO_6 octahedra forming Ir_3O_{12} clusters that are vertex linked to construct one-dimensional (1D) chains along the *c* axis.[4–6] $BaIrO_3$ is isostructural to metallic $BaRuO_3$,[5] but the monoclinic distortion in $BaIrO_3$ generates twisting and buckling of the cluster trimers that give rise to two 1D zigzag chains along the *c* axis and a layer of corner sharing IrO_6 octahedra in the *ab* plane, bringing about both 1D and two-dimensional (2D) structural characteristics.[4–6] It is the distortions in the structure that lead to insulating behavior; the resistivity is further drastically increased by substituting Ca for Ba, at the few percent level, which introduces additional structural distortions.[7]

Magnetization measurements have demonstrated a magnetic-field insensitive ferromagnetic transition at $T_{c3}=175$ K, and the *c*-axis resistivity reveals several features: at high temperatures the behavior is nonmetallic ($d\rho_c(T)/dT<0$), with a discontinuity visible at T_{c3}; at $T_{c2}\simeq 80$ K the resistivity peaks and the behavior is metallic on cooling ($d\rho_c(T)/dT>0$) until a Mott-like transition is encountered at $T_{c1}=26$ K.[3] Nonlinear conductivity and the opening of an optical gap are consistent with CDW formation accompanying the ferromagnetic ordering. This interpretation is supported by results of tight-binding band-structure calculations,[8] which show partially nested pieces of a Fermi surface that could signify the formation of a CDW state. The saturation moment associated with the Ir ions, $0.03\mu_B$, is very small compared to the expected moment for a $5d$,[5] $S=1/2$ ion. It has been proposed[3,8] that the small moment is an intrinsic property caused by *d-p* hybridization and small exchange splitting rather than spin canting from a localized antiferromagnetic configuration. The addition of small amounts of Sr dopant into the material has been shown to strongly suppress the ferromagnetic transition while increasing the Ir saturation moment and inducing a nonmetal-metal transition at high temperatures.[7]

Muon-spin relaxation (μSR) is an extremely sensitive probe of magnetism, well suited to studying the spin order and dynamics arising from the small Ir moment; neutron scattering studies of iridates are hindered by the large neutron absorption cross section of Ir. In order to provide a unique insight into the magnetic properties at a local level, we performed μSR measurements on a powdered sample of $BaIrO_3$, studying the ferromagnetic transition at T_{c3} and the additional transitions[3] observed on cooling. The experiments were carried out using the general purpose surface-muon (GPS) instrument at the Swiss Muon Source, Paul Scherrer Institute, Villigen, Switzerland. In these μSR experiments, spin-polarized positive muons (μ^+, mean lifetime 2.2 μs, momentum 28 MeV/*c*) were implanted into a powder sample of $BaIrO_3$ prepared as described in Ref. 4. The muons stop quickly (in $<10^{-9}$ s), without significant loss of spin polarization. The time evolution of the muon spin polarization can be detected by counting emitted decay positrons forward (*f*) and backward (*b*) of the initial muon spin direction, due to the asymmetric nature of the muon decay.[9] In our experiments we record the number of positrons detected by forward (N_f) and backward (N_b) scintillation counters as a function of time and calculate the asymmetry function, $A(t)$, using

$$A(t)=\frac{N_f(t)-\alpha_{\mathrm{exp}}N_b(t)}{N_f(t)+\alpha_{\mathrm{exp}}N_b(t)}, \tag{1}$$

where α_{exp} is an experimental calibration constant and differs from unity due to nonuniform detector efficiency. The quan-

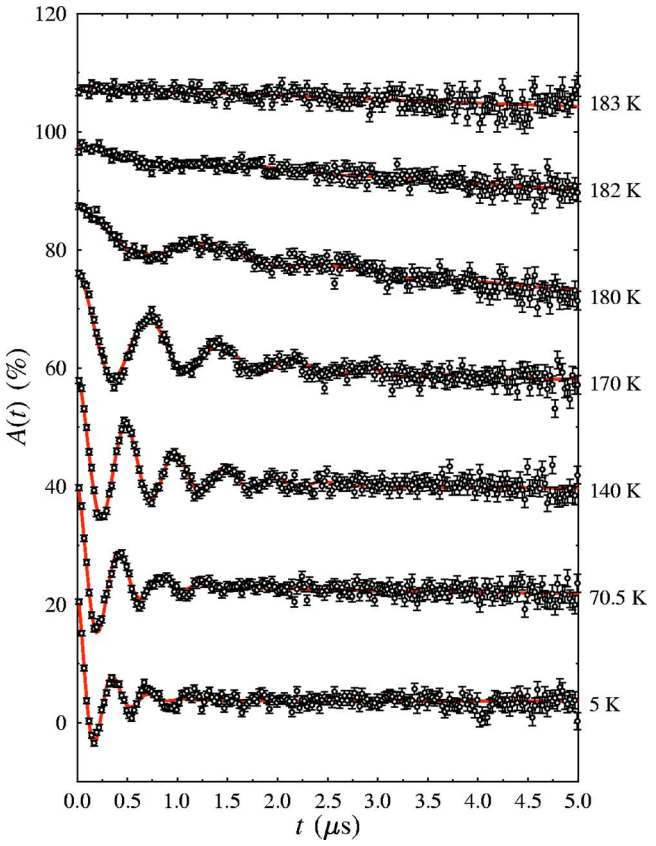

FIG. 1. (Color online) Typical muon asymmetry spectra measured at various temperatures. The 70, 140, 170, 180, 182, and 183 K spectra are offset by 18, 36, 54, 65, 75, and 85 % asymmetry, respectively. The solid (red) lines are fits to Eq. (2).

tity $A(t)$ is then proportional to the average spin polarization, $P_z(t)$, of muons stopping within the sample. The muon spin precesses around a local magnetic field, $\mathbf{B}_\mu$ (with a frequency $\nu_\mu=(\gamma_\mu/2\pi)|B_\mu|$, where $\gamma_\mu/2\pi=135.5$ MHz T^{-1}).

Typical muon asymmetry spectra for $BaIrO_3$ are shown in Fig. 1. Clear oscillations are visible for $T\lesssim 180$ K, and it was possible to fit the data to the function

$$A(t) = A_{\mathrm{bg}} + A_{\mathrm{rel}} \exp(-\lambda_{\mathrm{rel}} t) + A_{\mathrm{osc}} \exp(-\lambda_{\mathrm{osc}} t)\cos(\gamma B_\mu t) \tag{2}$$

over the entire temperature range studied, where A_{bg} represents a time-independent background due to muons stopping in the silver foil that surrounds the sample; λ_{rel} and A_{rel} are the exponential relaxation rate and amplitude of a relaxing fraction; and λ_{osc} and A_{osc} are the damping rate and amplitude of an oscillating fraction. The parameters extracted from these fits are shown in Fig. 2.

The magnitude of the magnetic field at the muon site is shown in Fig. 2(a). It begins to grow smoothly on cooling below T_{c3}, but undergoes an anomalous change near T_{c1}. The muon is able to detect changes to the local magnetization that are not detectable by bulk probe measurements (such as magnetization). The B_μ data were fitted, for $T>50$ K (in order to avoid the anomaly), to the phenomenological equation

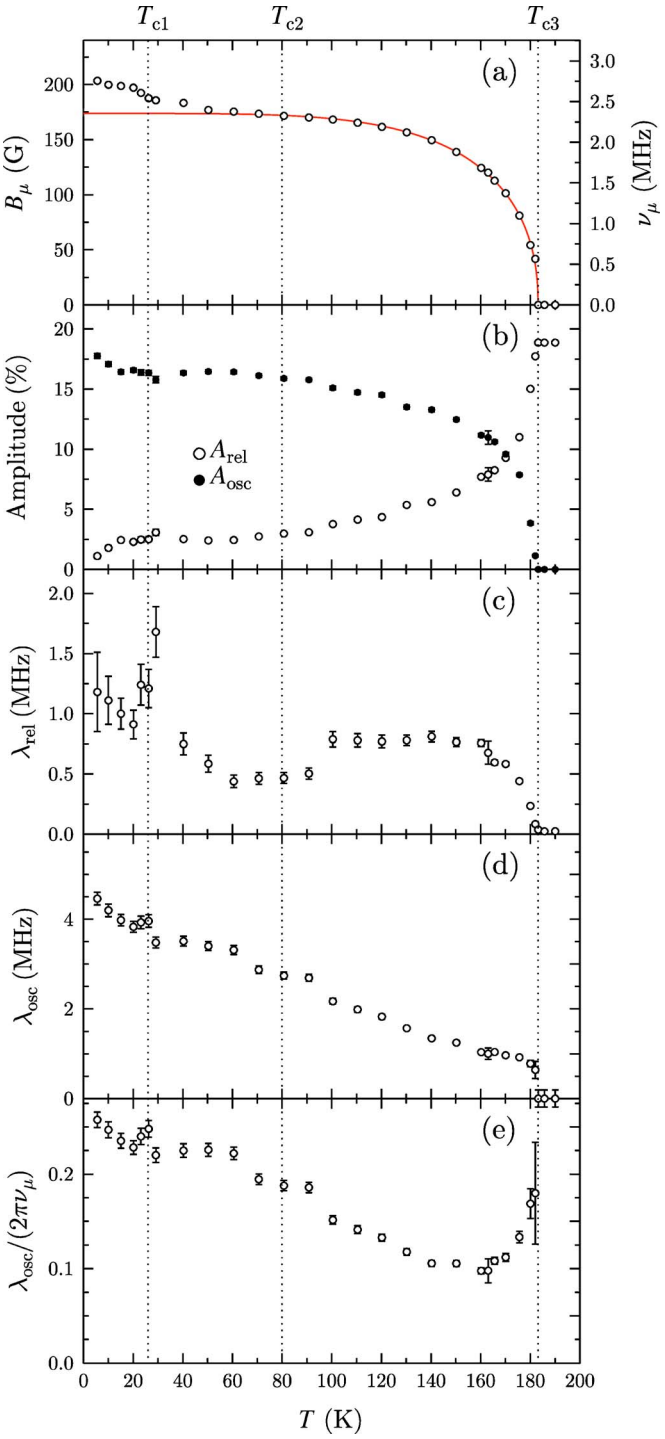

FIG. 2. Parameters extracted from fits of data to Eq. (2). (a) The magnitude of the magnetic field at the muon site and a fit to Eq. (3) (solid line). (b) The relaxing amplitude associated with the oscillating (closed symbols) and the relaxing (open symbols) fractions. (c) The exponential relaxation rate (λ_{rel}). (d) The oscillation damping rate (λ_{osc}). (e) The ratio $\lambda_{\mathrm{osc}}/2\pi\nu_\mu$, which is a measure of the local magnetic inhomogeneity. The dashed vertical lines mark the positions of T_{c1}, T_{c2}, and T_{c3}.

TABLE I. Values of parameters extracted from fitting B_μ to Eq. (3).

Parameter	Value
$B_\mu(0)$ (Gauss)	173.7(7)
T_{c3} (K)	183.12(4)
α	4.5(1)
β	0.435(8)

$$B_\mu(T) = B_\mu(0)\left[1 - \left(\frac{T}{T_{c3}}\right)^\alpha\right]^\beta, \quad (3)$$

and while the fit is good at high temperatures, there are clear departures at low temperature [Fig. 2(a)]. The extracted parameters are shown in Table I and the fitted curve is shown in Fig. 2(a) as a solid line. Our sample shows $T_{c3} \simeq 183$ K (from both μSR and magnetization, see below), which is a little higher than that reported previously,[3] perhaps reflecting the high purity of our sample.

A better understanding of the critical behavior near T_{c3} can be gained from the scaling analysis, shown in Fig. 3, which reveals that data for temperatures near to T_{c3} fit well to a power law, whose gradient on the log-log plot gives $\beta = 0.40(3)$, close to 0.367 expected for three-dimensional Heisenberg behavior. The point nearest to T_{c3} is poorly fitted; this is likely due to uncertainty in our value for T_{c3}.

The internal field at the muon site is very much smaller (by a factor of ~30) than that measured in other magnetic oxides (see, e.g., Refs. 10 and 11) in which the metal ion possesses its full moment. This is strong experimental evidence for a very small Ir magnetic moment in $BaIrO_3$, and rules out the possibility[12] that the weak ferromagnetism arises from the canting of antiferromagnetically arranged

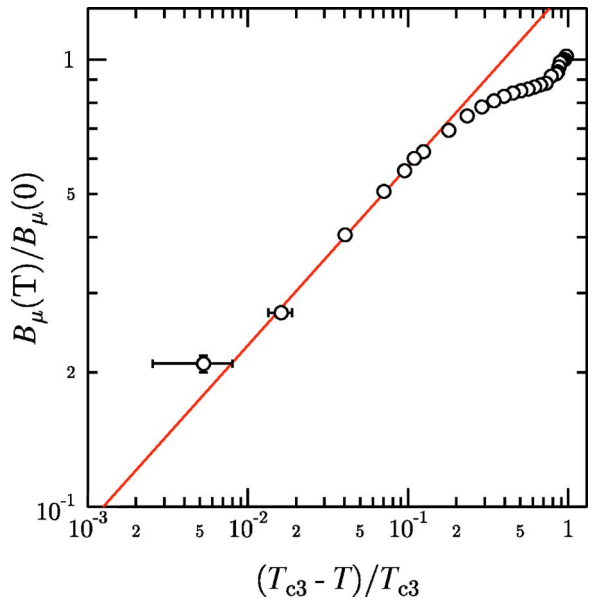

FIG. 3. Plot of scaled B_μ against scaled temperature (using $T_{c3} = 183$ K), showing a fit to points in the critical region, yielding a magnetization scaling parameter β of 0.40(3).

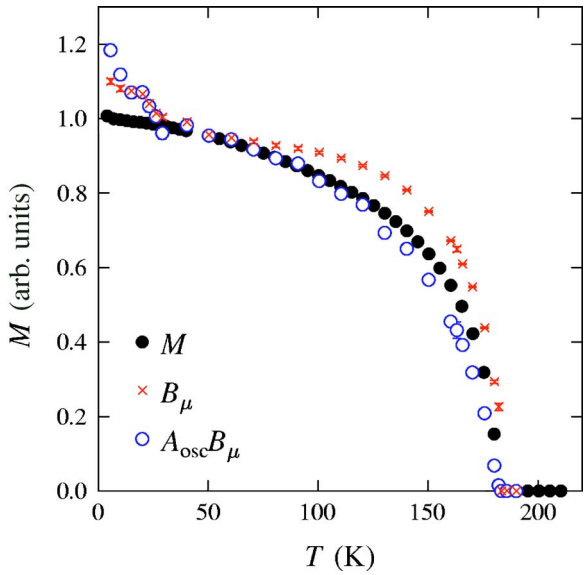

FIG. 4. Scaled measurements of magnetization: field-cooled (100 Oe) magnetization for a powder sample of $BaIrO_3$ measured in a SQUID (filled circles); field at the muon site B_μ (crosses); and $A_{osc}B_\mu$ (open circles).

spins. Below a temperature close to T_{c1}, B_μ departs sharply from the magnetization data, showing that the Fermi surface rearrangement that occurs at T_{c1} leads to a slight redistribution of the internal moment distribution inside the unit cell, possibly between different Ir ions.

The amplitude of the oscillating signal A_{osc} is expected to be proportional to the volume fraction of the magnetically ordered phase, and for a conventional magnetic transition would be zero above the transition, and nonzero and constant below it (see, e.g., Ref. 13). In Fig. 2(b), it is seen to grow slowly as the temperature is reduced below T_{c3}. Thus it is not only the size of the Ir moment, proportional to B_μ, which grows as the sample is cooled, but also the fraction of the sample that is magnetically ordered.

A comparison of the various measures of the magnetization is shown in Fig. 4. The bulk magnetization was measured after field cooling in 100 Oe in a Quantum Design MPMS superconducting quantum interference device (SQUID) magnetometer, and the resulting (normalized) curve is seen to be significantly below the corresponding B_μ curve over a large range of temperature. Also shown is the result of multiplying each B_μ value by its corresponding amplitude fraction A_{osc}, which is expected to be proportional to the average magnetization; this curve is a better (though not perfect) match to the bulk measurement data. The bulk magnetization results from an ordered fraction whose order parameter increases at the same time as its volume grows. Since the bulk magnetization was measured in a field, it might be expected to lie slightly above the $A_{osc}B_\mu$ curve, which was measured in zero applied field. We note that because the ordered fraction grows as the sample is cooled below T_{c3}, extracting a critical exponent such as β from either magnetization data or from the height of a neutron Bragg peak would not be a reliable procedure for determining intrinsic properties, whereas muons probe directly the

properties of the ordered fraction. It may be possible that the increase of the magnetic fraction with decreasing temperature, as parametrized by A_{osc}, reflects the nucleation of weak ferromagnetically ordered regions between isolated nonmagnetic Ir(III) centers, since the synthesis is believed to lead to $BaIrO_{3-\delta}$ with $\delta \sim 0.04$.

The exponential relaxation rate λ_{rel} reflects the dynamics of the field at the muon site(s) and is shown in Fig. 2(c). A large peak is expected near a magnetic phase transition due to the critical slowing down of spin dynamics, but is not visible near T_{c3}. It is strongly suppressed because only a tiny fractional volume of the sample is locally ordered at the transition temperature. A large peak is, however, seen at T_{c1}. Temperature T_{c2} is barely evident in the measured data: it seems to have no effect on $B_\mu(T)$, but possibly appears in λ_{rel} as a small step near $T=95$ K.

The oscillation damping rate λ_{osc} [shown in Fig. 2(d)] is proportional to the width of the ordered field distribution that gives rise to the oscillating signal, and is seen to rise as the temperature is lowered below T_{c3}. It has an almost linear dependence on temperature, and seems insensitive to the transitions at T_{c1} and T_{c2}. In more conventional magnets this rate peaks near the transition and becomes smaller on cooling as the order becomes more uniform and static. The temperature dependence of the local magnetic inhomogeneity, quantified by the ratio $\lambda_{osc}/(2\pi\nu_\mu)$ is shown in Fig. 2(e) and shows that, at least in the environment of the muon site, the system becomes progressively more magnetically inhomogeneous on cooling, in direct contrast to the behavior observed in most ferromagnetic systems.

In summary, we have used μSR to follow the development of magnetic order in $BaIrO_3$ from a local viewpoint. Our experiments show that the weakly ferromagnetic state, formed alongside the CDW state on cooling below T_{c3}, demonstrates unusual behavior in the development of the magnetically ordered volume fraction and the longitudinal and transverse relaxation rates. This, together with the very low frequency of the muon oscillation, leads us to conclude that the weak magnetism arises because of small exchange splitting, and is primarily driven by the changes at the Fermi surface that lead to the formation of the CDW state. In addition, a small anomalous change is seen in the local magnetic field (but not the bulk magnetization) at the Mott-like transition at T_{c1}, and is likely due to a local rearrangement of the magnetic moments caused by further changes at the Fermi surface. Evidence for the metal-insulator transition at T_{c2} is missing from both specific heat data[14] and our own μSR data, supporting the suggestion[3] that T_{c2} is a crossover point between partial Fermi surface gapping at T_{c3} and full gapping at T_{c1}, rather than a true phase transition.

Parts of this work were performed at the Swiss Muon Source, Paul Scherrer Institute, Villigen, Switzerland. We are grateful to H. Luetkens and A. Amato (PSI) for experimental assistance, to M.-H. Whangbo (North Carolina State University) for useful discussions concerning his tight-binding calculations, and to the EPSRC (UK) for financial support.

[1] E. Ohmichi, Y. Yoshida, S. I. Ikeda, N. Shirakawa, and T. Osada, Phys. Rev. B **70**, 104414 (2004).

[2] F. Nakamura, T. Goko, M. Ito, T. Fujita, S. Nakatsuji, H. Fukazawa, Y. Maeno, P. Alireza, D. Forsythe, and S. R. Julian, Phys. Rev. B **65**, 220402(R) (2002).

[3] G. Cao, J. E. Crow, R. P. Guertin, P. F. Henning, C. C. Homes, M. Strongin, D. N. Basov, and E. Lochner, Solid State Commun. **113**, 657 (2000).

[4] A. V. Powell and P. D. Battle, J. Alloys Compd. **191**, 313 (1993).

[5] A. Gulino, R. G. Egdell, P. D. Battle, and S. H. Kim, Phys. Rev. B **51**, 6827 (1995).

[6] T. Siegrist and B. L. Chamberland, J. Less-Common Met. **170**, 93 (1991).

[7] G. Cao, X. N. Lin, S. Chikara, V. Durairaj, and E. Elhami, Phys. Rev. B **69**, 174418 (2004).

[8] M.-H. Whangbo and H.-J. Koo, Solid State Commun. **118**, 491 (2001).

[9] S. J. Blundell, Contemp. Phys. **40**, 175 (1999).

[10] A. I. Coldea, S. J. Blundell, C. A. Steer, J. F. Mitchell, and F. L. Pratt, Phys. Rev. Lett. **89**, 277601 (2002).

[11] R. H. Heffner, J. E. Sonier, D. E. MacLaughlin, G. J. Nieuwenhuys, G. M. Luke, Y. J. Uemura, William Ratcliff II, S.-W. Cheong, and G. Balakrishnan, Phys. Rev. B **63**, 094408 (2001).

[12] R. Lindsay, W. Strange, B. L. Chamberland, and R. O. Moyer, Solid State Commun. **86**, 759 (1993).

[13] K. H. Chow, P. A. Pattenden, S. J. Blundell, W. Hayes, F. L. Pratt, T. Jestädt, M. A. Green, J. E. Millburn, M. J. Rosseinsky, B. Hitti, S. R. Dunsiger, R. F. Kiefl, C. Chen, and A. J. S. Chowdhury, Phys. Rev. B **53**, R14725 (1996).

[14] G. Cao, G. Shaw, and J. W. Brill, J. Phys. IV **12**, 91 (2002).